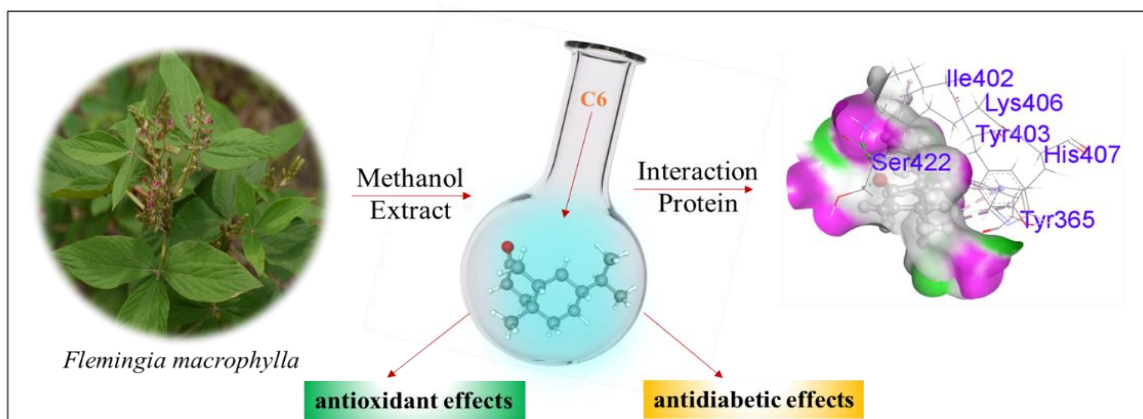# Antioxidant and Antidiabetic Effects of *Flemingia macrophylla* Leaf Extract and Fractions: *In vitro*, Molecular Docking, Dynamic Simulation, Pharmacokinetics, and Biological Activity Studies

Kaniz Fatema,[a,c] Ayesha Akter Sharmin,[a] Jinat Fatema Sharna,[a,c] Md. Anamul Haque,[a,c,*] Mst. Mahfuza Rahman,[a] Shahin Sarker,[b] Mohsin Kazi,[d] Md. Rezaur Rahman,[e,*] Murtala Namakka,[e] Monir Uzzaman,[c,f] and Md Abdul Majed Patwary [g,*]

* Corresponding authors: rmrezaur@unimas.my; anamul@cou.ac.bd (M.A.H.); mamajedp@gmail.com (M.A.M.P.)

GRAPHICAL ABSTRACT

Antioxidant and Antidiabetic Effects of *Flemingia macrophylla* Leaf Extract and Fractions: *In vitro*, Molecular Docking, Dynamic Simulation, Pharmacokinetics, and Biological Activity Studies

Kaniz Fatema,[a,c] Ayesha Akter Sharmin,[a] Jinat Fatema Sharna,[a,c] Md. Anamul Haque,[a,c,*] Mst. Mahfuza Rahman,[a] Shahin Sarker,[b] Mohsin Kazi,[d] Md. Rezaur Rahman,[e,*] Murtala Namakka,[e] Monir Uzzaman,[c,f] and Md Abdul Majed Patwary [g,*]

Flemingia macrophylla has traditionally been applied to relieve inflammation, diabetes, and circulatory complications. The leaf extract of *F. macrophylla* and its fractions were investigated for their *in-vitro* antioxidant and anti-diabetic properties. The phytochemical screening showed valuable phytochemicals, including glycosides, flavonoids, saponins, *etc.* GC–MS analysis of the phytochemicals in the methanol extract detected 19 bioactive compounds. Among the diverse fractions, the ethyl acetate fraction (EFM) exhibited the highest phenol and flavonoid contents of 557 mg GAE/g and 326 mg QCE/g, respectively. The total antioxidant content of EFM was found to be 292.41±19.16 mg AAE/g, while its antidiabetic study showed the greatest level of α -glucosidase (IC$_{50}$: 11.27±1.25 µg/mL) and α -amylase (IC$_{50}$: 10.04±0.63 µg/mL) inhibitory effects. The docking results showed that C6 had the highest binding scores of -9.0, -7.4, and -7.6 kcal/mol against antioxidant (6NGJ), α-glucosidase (5NN5), and α-amylase (4GQR) proteins, respectively. The dynamics simulation disclosed that C6-receptor protein complexes remained stable at the binding pocket under human body conditions and retained their stiff morphology for 100 nanoseconds (ns). ADMET results demonstrated their noncarcinogenic and well-absorbed properties, where PASS prediction data confirmed their efficacy as an antioxidant, antiulcerative, thrombolytic, and antidiabetic. Therefore, *F. macrophylla* has potential health benefits.

INTRODUCTION

Natural products are usually secondary metabolites produced by organisms in response to environmental contexts such as illness, competition, and dietary changes. Approximately 35% of medicines are made using natural ingredients (Calixto 2019). Free radicals are necessary for mitochondrial respiration and metabolism (Kumar *et al*. 2014). By causing redox reactions, these free radicals, which are much more sensitive than oxygen molecules, can cause damage to biomacromolecules such as nucleic acids, proteins, and lipids (Iriti and Faoro 2008). When normal antioxidant protection and repair systems of the human body cannot eliminate the state of peroxidation, it can lead to bad outcomes such as DNA damage, cell death, cancer, and aging (Bakri *et al.* 2024). Antioxidants protect biomolecules, proteins, sugars, and triglycerides (Umesha *et al*. 2013). They reduce cell and tissue damage by avoiding or delaying oxidation (Fındık *et al*. 2011).

Diabetes mellitus is one of the most serious diseases that affect most of the world's population (Alsolami *et al.* 2023). It is linked to hyperglycemia due to a full or relative lack of insulin result or action. Long-term hyperglycemia damages valuable organs, including the retina, kidney, heart, and blood vessels (Alam *et al*. 2014). Traditional medicine praises herbal antidiabetic medications, but they have not been marketed. Enzymes that break down starch tend to be reduced in a body that is suffering from diabetes. Dietary glucose release causes postprandial hyperglycemia. In addition, α-amylase and α-glucosidase break down polysaccharides into monosaccharides. To reduce postprandial hyperglycemia, one promising technique is to slow glucose uptake by blocking α-glucosidase and α-amylase, which are important carbohydrate metabolizing enzymes (Arumugam *et al*. 2013).

Charchara is the local name for the woody shrub *F. macrophylla*, which belongs to the Fabaceae family. This plant has been used historically for a variety of purposes, including the relieving of inflammation and diabetes, as well as the improvement of blood circulation (Begum *et al*. 2013). In the northeastern region of India it is traditionally used as a folk remedy by practitioners for its hypoglycemic and antidiabetic activity (Syiem and Khup 2007). Kabir *et al*. (2015) conducted a study on the computational prediction of the ability of isolated chemicals from *F. macrophylla* to dissolve blood clots, as well as their interaction with target molecules. Shahadat *et al*. (2015) investigated the antipyretic and *in vivo* analgesic properties of *F. macrophylla* in Swiss albino mice, as well as its *in vitro* anti-inflammatory activity. Hsieh *et al*. (2011) also investigated the hepatoprotective influence of the aqueous extract of *F. macrophylla* in rats. The present article reports a comprehensive study of *F. macrophylla* leaf extract and four fractions using both computer-simulated and experimental analyses to recognize the properties of the key active constituents to examine the potential health benefits and evaluate the antioxidant, and in-vitro antidiabetic potential.

EXPERIMENTAL

Chemical Reagents

In this investigation, methanol, 2,2-diphenyl-1-picrylhydrazyl (DPPH), ascorbic acid, and Mayer's reagents were purchased from Merck (Darmstadt, Germany). Ferric ammonium molybdate, potassium ferricyanide, trichloroacetic acid, DNSA reagent, α-glucosidase, and α-amylase, were obtained from Sigma Chemicals Co. (St. MO, USA). All the reagents as well as chemicals were of the highest chemical and analytical grade.

Leaf Extraction and Fractionation

In two amber-colored containers, 2.5 L of methanol was poured into 500 g of powdered leaves in each with 14 days of occasional shaking (50 rpm) followed by filtration. To remove the solvent, a rotary evaporator was utilized. After removing the solvent, *F. macrophylla* generates a greenish-black gummy concentration. The Kupchan method was applied to the methanol extract (MFM) to obtain petroleum ether (PFM), dichloromethane (DFM), ethyl acetate (EFM), and water (WFM) fractions (Kupchan and Tsou 1973). Finally, the extract and fractions were dried and stored for further applications.

Preliminary Phytochemical Screening

Earlier developed methods of phytochemical assessment were applied for freshly prepared extract and fractions to screen steroids, resins, anthraquinones, tannins, phlobatanins, saponins, glycosides, alkaloids, and flavonoids (Tripathi and Mishra 2015; Odeja *et al*. 2017; Bayero *et al*. 2019).

Quantitative Analysis of Leaf Extract and Fractions

Total phenol content (TPC)

The TPC was determined using a modified Folin-Ciocalteu technique (Wolfe *et al*. 2003). An aliquot of the standard/extract/fractions (50, 100, 200, and 400 µg/mL) was mixed with 4 mL of Na_2CO_3 solution and 2 mL of Folin-Ciocalteu reagent. To achieve the appropriate color, the tubes were vortexed vigorously for 20 min at 25 °C. A UV spectrophotometer was employed to identify absorbance at 756 nm. Gallic acid (standard, GA), equivalents (GAE), or mg of GA/g of dry extract, was employed to calculate the phenol content (Rahman *et al*. 2015).

Total flavonoid content (TFC)

The approach developed by Brighente *et al*. (2007) was utilized to assess the TFC. Two mL of the extract, fractions, and standard were added with an equivalent volume of 2% w/v $AlCl_3.6H_2O$ solution. The mixture was stirred quickly, and after one hour of incubation at 20 °C, the absorbance at 415 nm was recorded by using a UV spectrophotometer. The results were calculated using a quercetin (QC) calibration curve and are expressed as mg QCE/gram of dry extract (Kasangana *et al*. 2015).

In-vitro Antioxidant Effect

Total antioxidant content (TAC)

TAC was measured with a UV-spectrophotometer and the phosphomolybdenum assay, as per reference (Prieto *et al*. 1999). Briefly, 2.7 mL of phosphomolybdenum reagent and 0.3 mL of a 1 mg/mL extract/fraction/ascorbic acid (AA) solution were mixed in a test tube with 28 mM Na_3PO_4 and 4 mM ammonium molybdate in 0.6 M H_2SO_4 acid. After a 90-min incubation period at 95 °C in a water bath, absorbance at 695 nm was measured against a blank (0.3 mL methanol) (Kasangana *et al*. 2015).

DPPH radical scavenging effect

The DPPH free radical-scavenging test was applied to evaluate the free radical-scavenging capacity identified by Blois (1958) and Demarchelier *et al*. (1997). Plant extracts decolorize DPPH methanol mixtures. Antioxidants cause DPPH to yellow, which appears violet or purple in methanol solution. Here, 1.6 mL of extract or fraction solution

was combined with 2.4 mL of DPPH solution in methanol at various concentrations (ranging from 6.25 to 400 µg/mL). The samples were vortexed at room temperature (RT) (25-26 °C) with a 30-min break in the dark before the absorbance at 517 nm was recorded (Rahman *et al*. 2015). The DPPH radical scavenging activity was determined by Eq. 1 (Rahman *et al*. 2022).

$$\% \text{ of free radical scavenging activity} = \frac{(A_{control} - A_{sample})}{A_{control}} \times 100 \qquad (1)$$

Ferric reducing capacity test (FRCT)

The ferric-reducing capacity of the sample was adjusted using Oyaizu's technique (Oyaizu 1986). The Perl technique was used to calculate the amount of Fe^{2+} in the H_2O while taking Prussian blue concentration into account. First, 12.5 mL of sample/standard solutions (12.5 to 400 g/mL) was added to 0.2 mL of potassium buffer and 12.5 mL of $[K_3Fe(CN)_6]$ solution. The next step was to incubate the reaction mixtures at 50 °C for 20 min. Then, 2.5 mL of a 10% trichloroacetic acid solution was added to each test tube. Two milliliters of the supernatant were extracted by adding 2.5 mL of distilled H_2O and 0.5 mL of a 0.1% ferric chloride solution after the tubes had been centrifuged at 3000 rpm for 10 min. A UV spectrophotometer was employed to assess the absorbance of the solution against a blank at 700 nm. After that, the 50% effective concentration (EC_{50}) of each extract and standard component was determined (Rahman *et al*. 2015).

In-vitro Antidiabetic Test

In-vitro α-glucosidase inhibition assay

The glucosidase inhibition test was carried out using the method depicted by Elya *et al*. (2012). Plant extract and fraction solutions (10 to 100 µg/mL) were prepared in 5% dimethyl sulfoxide. Then, 80 µL of the sample or standard acarbose solution was combined with 20 µL of α-glucosidase solution (0.01 mg/mL). After 10 min of incubation at 37 °C, 50 µL of 5 mM p-nitrophenyl-D-glucopyranoside (p-NPG) was added to start the reaction. Then, 2.5 mL of 0.1 M Na_2CO_3 solution was added after 60 min of incubation at 37 °C. The absorbance at 400 nm was used to measure α-glucosidase activity (Alqahtani *et al*. 2019). The percentage of inhibition employed to define α-glucosidase inhibitory activity was calculated using a similar sort of Eq. 2, as follows:

$$\% \text{ of α-glucosidase/α-amylase inhibition} = \frac{(A_{control} - A_{sample})}{A_{control}} \times 100 \qquad (2)$$

In-vitro α-amylase inhibition assay

The technique depicted by Kwon *et al*. (2008) was utilized to determine the α-amylase inhibitory activity. Twenty mL of α-amylase solution (0.5 mg/mL) was added to 500 µL of extract/fractions or acarbose (standard), then combined with 500 µL of 20 mM sodium phosphate buffer at pH 6.8. The mixture was further incubated at 25 °C for 10 min. Each test tube was therefore loaded with 500 µL of a 1% starch solution in a 0.02 M sodium phosphate buffer at pH 6.9 and was again incubated at 25 °C for 15 min. Di-nitro salicylic acid (0.5 mL) was applied to stop the reaction. The test tubes were then cooled to room temperature after spending 5 min submerged in boiling water. The absorbance at 540 nm was measured after diluting the reaction mixture with 10 mL of distilled H_2O. Following Eq. 2, the percentage of inhibition employed to express the α-amylase inhibitory activity was determined. The crude extract, solvent fractions, and acarbose IC_{50} values were

determined using the dose-response curve, which was interpolated using the linear regression analysis (Alqahtani *et al*. 2019).

GC–MS Analysis

GC–MS analysis was employed on the methanol extract using a GCMS-QP2020 (Shimadzu, Japan). The analysis was conducted using an RTX-5 MS capillary column (30 m x 0.25 mm x 0.25 µm) that had a cross band of 5% diphenyl-95% dimethylpolysiloxane. Herein, 1.72 mL/min of helium (99.99%) was employed as the carrier gas in this experiment. The temperature of the oven was initially set at 80 °C (isothermal for 2 min) and raised to 150 °C at a rate of 5 °C (kept for 3 min). After raising the temperature by 5 °C per min and holding it for 5 min, the oven's final temperature was 280 °C. The splitless injection of the sample (1 µL) was performed at 50:0 with an injection temperature of 220 °C. The whole duration of the run was 50 min. An ionizing potential of 70 eV was utilized to guarantee electron-impact ionization, and the ion source was adjusted to 280 °C. The mass spectra were found in the 45-350 (*m/z*) scan range, and their components were identified using a probability-based approach by comparing them to the spectra of known compounds stored in the NIST08.LIB database (Gomathi *et al*. 2015).

Computational Analysis

Preparation of ligands and proteins, docking, and nonbonding interactions

The structures of six significant compounds identified in leaf extract were determined employing GC–MS and denoted as C1, C2, C3, C4, C5, and C6, as shown in Fig. 1.

i-Propyl 9-Octadecenoate (**C1**, 5356106)

n-Propyl 11-Octadecenoate (**C2**, 87131822)

n-Hexadecanoic Acid (**C3**, 985)

Supraene (**C4**, 638072)

Neophytadiene (**C5**, 10446)

2(1H)-Naphthalenone, Octahydro-4a-Methyl-7-(1-methylethyl)- (**C6**, 41133)

Ascorbic acid (**AA**, 54670067)
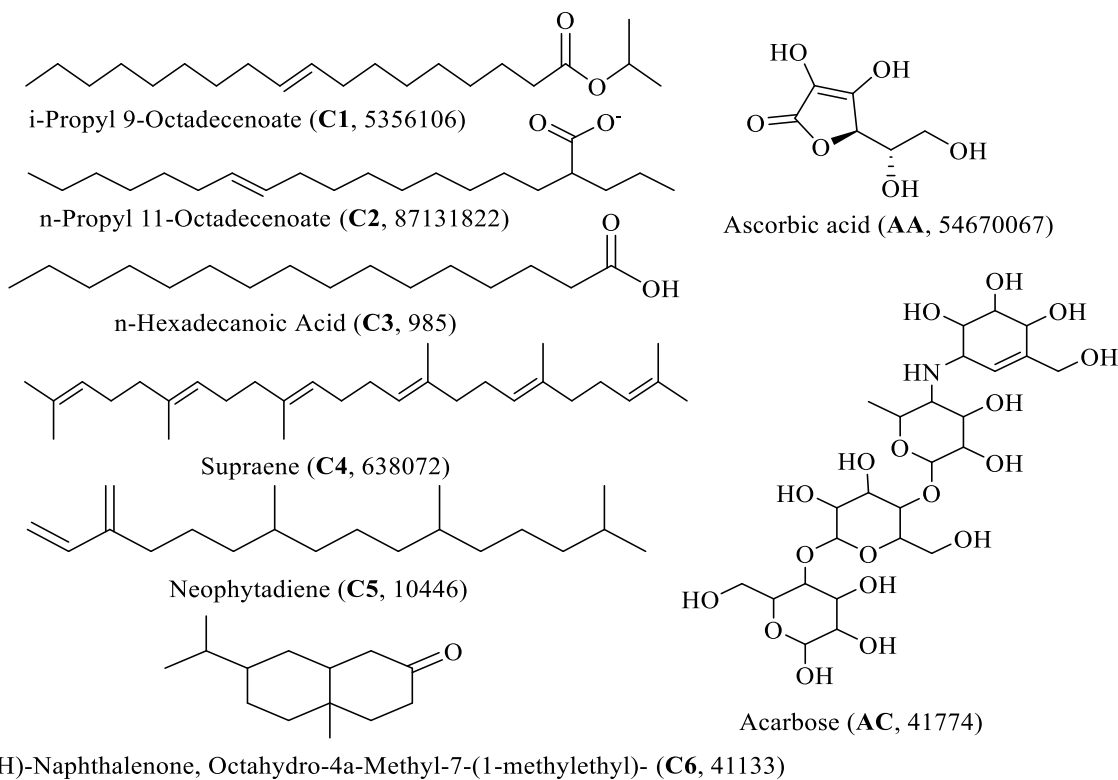
Acarbose (**AC**, 41774)

Fig. 1. Chemical structures of AA, AC, and six particular compounds with PubChem ID

Besides, the standard drugs ascorbic acid (AA) and acarbose (AC) were used to relate the binding affinity as well as nonbonding interactions. By operating the Gaussian 09 W software package using density functional theory (DFT), the geometry optimization was accomplished in the presence of B3LYP (Rupa *et al*. 2022) hybrid functionals using Pople's 6-31G (d, p) basis set (Sure *et al*. 2014). The Protein Data Bank (PDB) format was used to acquire the three-dimensional structure of the protein from the RCSB (Rose *et al*. 2016). These structures contain antioxidants (PDB ID: 6NGJ) (Do *et al*. 2019), antidiabetic α-glucosidase (PDB ID: 5NN5) (Roig-Zamboni *et al*. 2017), and α-amylase (PDB ID: 4GQR) (Williams *et al*. 2012), receptor proteins, respectively. To eliminate unwanted heteroatoms, chains, H_2O molecules, and co-crystallized ligands, PyMOL (Version 1.7.4) was utilized. In order to decrease the chain energy and remove superfluous protein interactions, the Swiss PDB reader (Version 4.1.0) was employed. Lastly, the 6NGJ, 5NN5, and 4GQR proteins were docked in a flexible fashion using the PyRx (Version 0.8) program. The medication is considered as the ligand, while protein works as macromolecules. The center grid boxes along the x, y, and z axes were preserved at 53.87, 70.63, and 58.28 Å for 6NGJ, 82.95, 79.57, 80.19 Å for 5NN5, and 58.99, 78.20, 58.54 Å for 4GQR protein, respectively. For nonbonding interactions, the drug and protein were saved as a single PDB file after docking and placed into BIOVIA Discovery Studio 2021.

Molecular Dynamics (MD) Simulation

Using the AMBER14 force field, the MD simulation of the docked complexes was carried out in YASARA dynamics (Uzzaman *et al*. 2021). The docked complexes underwent cleaning, and the mechanism that was responsible for the H-bond network was orientated. A cubic simulation cell was employed, utilizing a TIP3P solvation mechanism. The physiological form of the complex was set as 298 K, 0.9% NaCl, and pH 7.4. The energy was minimized with the steepest gradient algorithm by the simulated annealing method. The time stage of the simulation was adjusted to 2 fs. The simulation trajectory was set to save after every 100 ps and extended to 100 ns. The radius of gyration, solvent accessible surface area (SASA), root mean square deviation (RMSD), and H-bond were all computed using the simulated trajectories (Krieger and Vriend 2015).

Pharmacokinetics, Biological Activity, and Drug-likeness Prediction

The ADMET (absorption, distribution, metabolism, excretion, toxicity) profile is crucial in medication design and analysis, since it considers both pharmacokinetic and pharmacodynamic factors. To have desirable and/or safe therapeutic impacts, a medicine must first be readily absorbed, then distributed uniformly throughout the body, and finally digested properly. The drug should leave the body within the predicted time range, whether through urine, feces, or other means. The AdmetSAR (Guan *et al*. 2019), and way2drug (Filimonov *et al*. 2014), and Swiss ADME web server were utilized for the pharmacokinetics and biological predictions.

Statistical Analysis

The three sets of data we obtained were presented along with their respective means, standard deviations, and interquartile ranges. The ANOVA was performed in SPSS version 15.0, and all charting was done in Graph Pad Prism version 6.0. The IC_{50} and EC_{50} values were computed using MS Excel-10.

RESULTS AND DISCUSSION

Preliminary Phytochemical Analysis

F. macrophylla leaf extracts and fractions showed saponins, steroids, flavonoids, alkaloids, resins, glycosides, and tannins in MFM, PFM, DFM, EFM, and WFM respectively. Table S1 shows that all extracts and fractions contained saponins, steroids, flavonoids, and anthraquinone. Alkaloids were absent in the MFM extract and PFM fraction, whereas phlobotannins were absent in the WFM, and the EFM fractions lacked glycosides. It is believed that plants contain a large number of phytochemicals; hence, a plant-based diet can aid in the prevention of many diseases (Mujeeb *et al.* 2014) agents, anti-inflammatories, anticoagulants, cardioprotective, sedatives, and hypotensive agents (Dey *et al.* 2020). However, plant-derived steroids are widely known for their cardiotonic and insecticidal activities. They are often used in medicine due to their well-known biological roles (Patel and Savjani 2015). As a resource of steroids and alkaloids, *F. macrophylla* can be used to heal various inflammatory conditions and cardiotonic diseases.

Total Phenol and Flavonoid Content

Phenols and flavonoids are the two most important secondary plant metabolites, which have unique biological activity as natural antibacterial agents and are superior to many other manufactured antibacterial agents (Bouyahya *et al*. 2016). The bulk of naturally occurring phenolic compounds, or flavonoids, are present in different plant sections both as glycosides and in free form. Numerous biological effects, including the prevention of angiogenesis, the suppression of mitochondrial adhesion, the antiulcer and antiarthritic properties, and the inhibition of protein kinase, have been found (John *et al*. 2014). The total phenolic compound in the MFM extract and fractions (PFM, DFM, EFM, and WFM) was raised in a concentration-dependent way, and gallic acid (GA) was utilized as a control. Fig. S3 depicts the extract and fractions, which were qualified in mg/gm of GAE. The TPCs for MFM, PFM, DFM, EFM, and WFM were in the following order at 400 µg/mL EFM > DFM > WFM > MFM > PFM, with 557.42±67.11, 443.55±26.82, 217.27±14.07, 86.31±40.74, and 41.87±26.67 mg/g (Table 1) [reported 43.8 ± 0.22 mg/g by ref (Begum *et al*. 2013). On the other hand, the EFM fraction contained a significantly higher flavonoid content (326.36±7.80 mg/g) than the DFM (214.11±12.84 mg/g), WFM (156.29±15.58 mg/g), MFM (84.87±17.52 mg/g) (Fig. S6) [reported 64.4 ± 0.56 mg/g by ref (Begum *et al.* 2 2013) fractions and PFM (47.45±5.10 mg/g) extract.

In-Vitro Antioxidant Effect

Total antioxidant content

The TAC was computed using the reduction of Mo(iv) and Mo(v) by the fractions and extract as well as the growth of a green phosphate/Mo(v) complex when the pH was acidic. It evaluates the antioxidants that are both H_2O and fat-soluble to determine their effectiveness (Jan *et al*. 2013). Table 1 depicts the highest value of TAC found from the EFM (292.41±19.16 mg/g), following DFM (274.84±2.34 mg/g), then WFM (203.21±4.68 mg/g), MFM (177.54±13.04 mg/g) extract, and the lowest value found from PFM (126.12±6.19 mg/g) fraction.

Table 1. TPC, TFC, TAC, IC_{50} (DPPH), EC_{50} (FRPT), and α-Glucosidase and α-Amylase Inhibitory Effects of Leaf Extracts and Fractions

Parameters		Standard, Extract, and Fractions of *F. macrophylla*				
	AC	MFM	PFM	DFM	EFM	WFM
TPC (mg/g) equivalent of GA	-	86.31±40.74	41.87±26.67	443.55±26.82	557.42±67.11	217.27±14.07
TFC (mg/g) equivalent of QC	-	84.87±17.52	47.45±5.10	214.11±12.84	326.36±7.80	156.29±15.58
TAC (mg/g) equivalent of AA	-	177.54±13.04	126.12±6.19	274.84±2.34	292.41±19.16	203.21±4.68
IC_{50} (DPPH) (µg/mL)	-	64.58±1.48	81.67±3.78	21.78±0.53	15.62±0.74	25.52±0.89
EC_{50} (FRPT) (µg/mL)	-	61.62±1.42	75.95±4.69	25.72±1.18	18.37±1.49	31.83±2.74
IC_{50} (α-glucosidase) (µg/mL)	5.45±0.19	24.01±1.49	32.66±0.99	14.82±1.03	11.27±1.25	18.74±0.90
IC_{50} (α-amylase) (µg/mL)	6.20±1.46	22.77±1.16	40.20±0.38	13.76±1.16	10.04±0.63	17.92±0.74

Note: Data are means ± SD, n=3, IC: inhibition concentration, EC: effective concentration

DPPH radical scavenging effect

The antioxidant activity can also be determined by the DPPH scavenging activity and ferric reducing activity because the antioxidant activity cannot be determined by a single procedure. DPPH is a strong free radical and is commonly employed for the assessment of the antioxidant activity of plant extracts (Ali *et al*. 2010). Herein, AA, EFM, DFM, WFM, MFM, and PFM each had IC_{50} values of 5.07±0.06, 15.62±0.74, 21.78±0.53, 25.52±0.89, 64.58±1.48, and 81.67±3.78 µg/mL, respectively (Table 1).

Ferric reducing capacity test (FRCT)

The FRCT assay of all the fractions, extract, and AA increased with a gradual rise in concentration. Reducing power is frequently used to assess a plant's ability to combat free radicals (Rahman *et al*. 2015). AA, a standard reducing agent, showed the highest absorbance (12.20±0.15 µg/mL) at concentrations ranging from 12.5 to 400 µg/mL. Among the extracts, EFM showed the maximum effect with an EC_{50} value of 18.37±1.49 µg/mL, and PFM showed the lowest effect with an EC_{50} value of 75.95±4.69 µg/mL (Table 1).

In Vitro Antidiabetic Test

In vitro α-glucosidase and α-amylase inhibition activity

Postprandial hyperglycemia can be reduced by inhibiting the activity of α-glucosidase and α-amylase in the intestinal and pancreatic tracts. This occurs as a direct result of the presence of additional carbs, which causes a delay in the digestion of absorbable monosaccharides (Kifle *et al*. 2021). The α-glucosidase and α-amylase inhibition activities are presented in Table 1. In this study, the EFM fraction showed the highest effect with IC_{50} values of 11.27±1.25 and 10.04±0.63 µg/mL for both α-glucosidase and α-amylase, respectively.

GC–MS Analysis

The GC–MS chromatogram of the methanol extract of *F. macrophylla* (Fig. 2) displayed 19 peaks, which indicates the presence of 19 phytochemicals. From the GC–MS data, benzene,1,3-dimethyl- had the shortest retention time (3.6 min), and 7-octylidenebicyclo [4.1.0] heptane had the longest (39.01 min) retention time. Likewise, (C1, 13.31%) and (C2, 9.04%) were the most common chemicals (Table 2). In this study, more bioactive components, such as C3, phytol, and tetradecanoic acid may have contributed to the enhanced antioxidant, anti-inflammatory, antiulcerative, and thrombolytic activity (Bodoprost and Rosemeyer 2007; Abirami and Rajendran 2011; Kala *et al*. 2011). Additionally, C4 has been linked to anticancer, antioxidant, chemo-preventive, gastroprotective, hepatoprotective qualities, pesticide, anti-tumor, and sunscreen capabilities. Previous studies have shown that octadecadienoic acid possesses anti-inflammatory, hypocholesterolemic, and antiarthritic effects (Gomathi *et al*. 2015) (Ponnamma and Manjunath 2012).
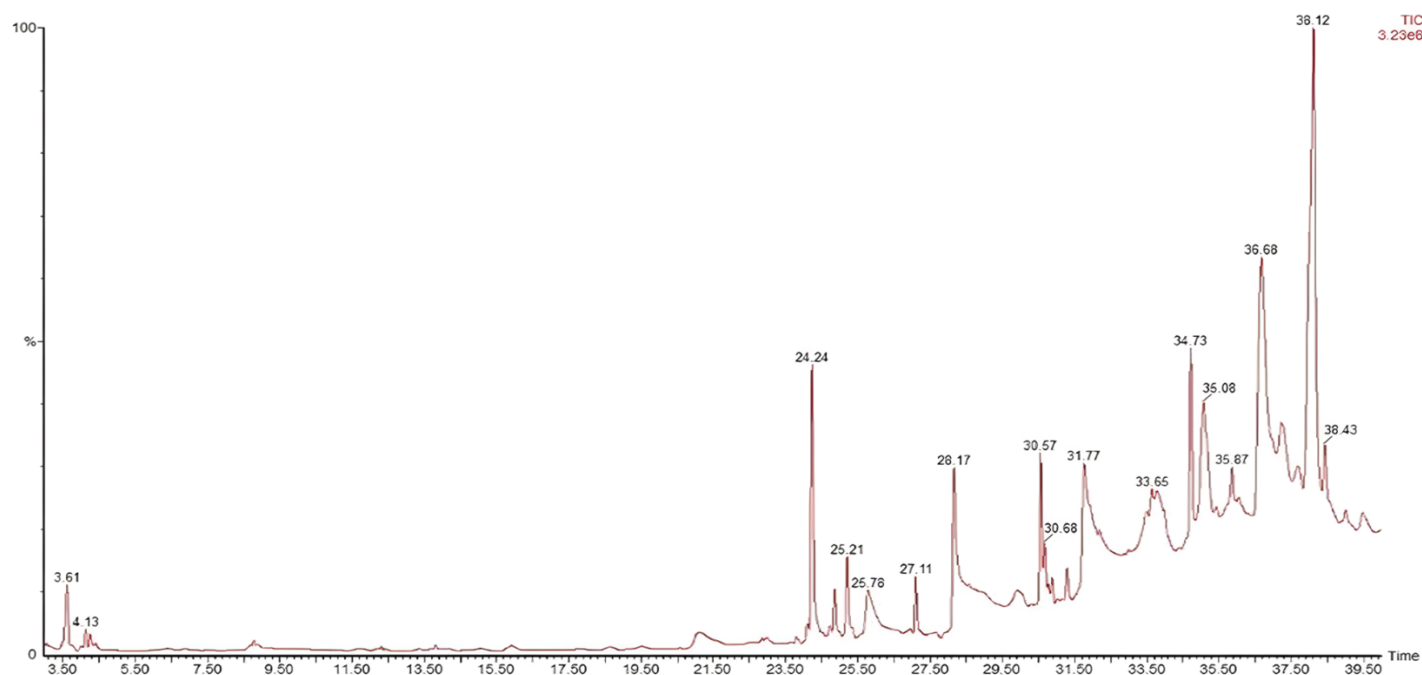
Fig. 2. GC–MS chromatogram of the methanolic extract

Table 2. GC–MS Analysis of the Leaf Extract of *F. macrophylla* in Methanol

ID	Bioactive Compounds	Retention Time	Molecular Weight	Peak Area (%)
01	Benzene, 1,3-Dimethyl-	3.6	106	0.93
02	Propanoic Acid, 2-Methylpropyl Ester	4.25	130	0.29
03	Hexadecane	8.78	126	0.48
04	Naphthalene	12.31	128	0.09
05	Hentriacontane	13.8	436	0.10
06	Neophytadiene (C5)	24.2	278	3.43
07	Phytyl Palmitate	24.8	534	0.59
08	Phytyl Tetradecanoate	25.2	506	0.86
09	Tetradecanoic Acid, 10,13-Dimethyl-,Methyl ester	27.11	270	0.60
10	n-Hexadecanoic Acid (C3)	28.2	256	6.70
11	Phytol	30.5	296	2.21
12	12,15-Octadecadienoic Acid, Methyl Ester	30.88	296	0.22
13	Methyl 2-Hydroxy-Octadeca-9,12,15-Trienoate	31.30	308	0.32
14	n-Propyl 11-Octadecenoate (C2)	31.78	324	9.04
15	Cis-Styryl Pentyl Sulfoxide	33.79	222	1.12
16	i-Propyl 9-Octadecenoate (C1)	36.68	324	13.31
17	Supraene (C4)	37.68	410	6.21
18	2(1H)-Naphthalenone, Octahydro-4a- Methyl-7-(1-methyl ethyl)- (C6)	38.43	208	2.46
19	7-Octylidenebicyclo [4.1.0] Heptane	39.01	206	0.56

Molecular Docking Simulation

The structure-based drug design approach known as molecular docking can predict how well a medication will bind to a receptor (Uzzaman *et al*. 2023). It is an important tool for hit recognition, lead improvement, and biological remediation, since the binding score and kind of drug-receptor protein interaction can be certainly assessed (Jannat *et al*. 2024), higher negative value indicates more tight binding with the receptor. Figure 3 presents a comprehensive overview of the binding affinity values with the antioxidant and antidiabetic potentials.
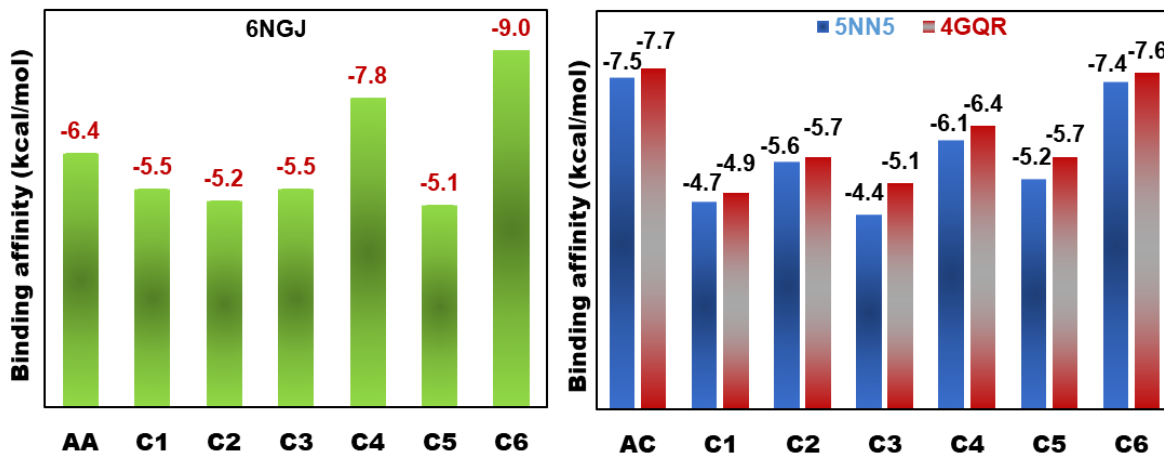

Fig. 3. Binding affinity of the selected compounds and standard drugs with (a) antioxidant (6NGJ), and (b) antidiabetic (5NN5) proteins, respectively

Docking and Non-bonding Interaction (NBI) against 6NGJ

In this study, the binding affinity of the considered standard drug (AA) was -6.4 kcal/mol, with the 6NGJ receptor, where C6 owed the highest binding score (-9.0 kcal/mol) with the same protein compared to other studied compounds. The C5 had a low binding score (-5.1 kcal/mol), indicating a weak binding with the respective protein (Fig. 3).
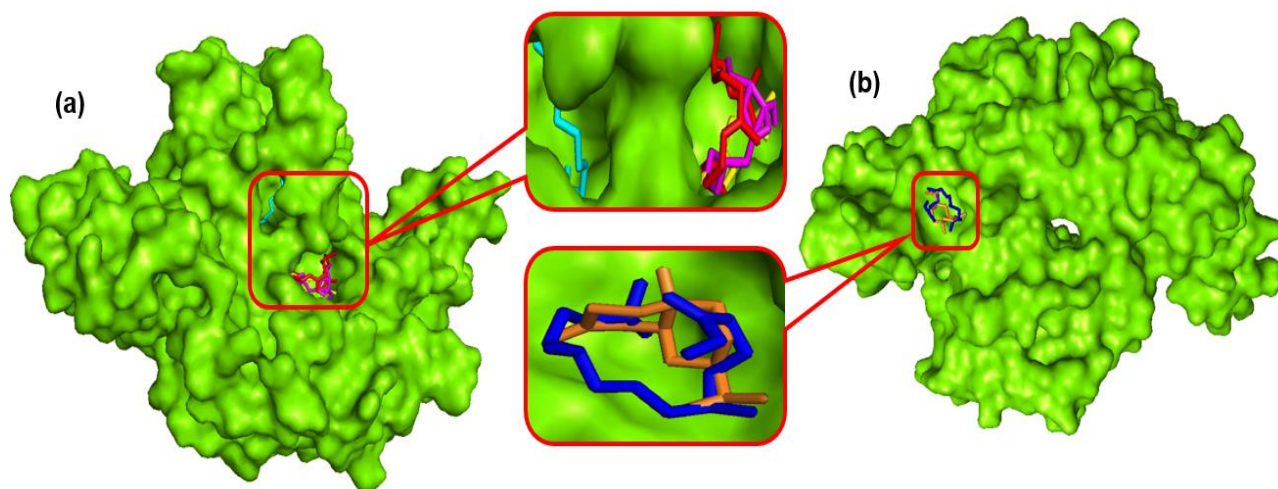

Fig. 4. (a) Surface outlook of the docked conformation of C1 (clay), C2 (magenta), C3 (yellow), C4 (red), and (b) C5 (blue), C6 (orange) at the binding site of the 6NGJ
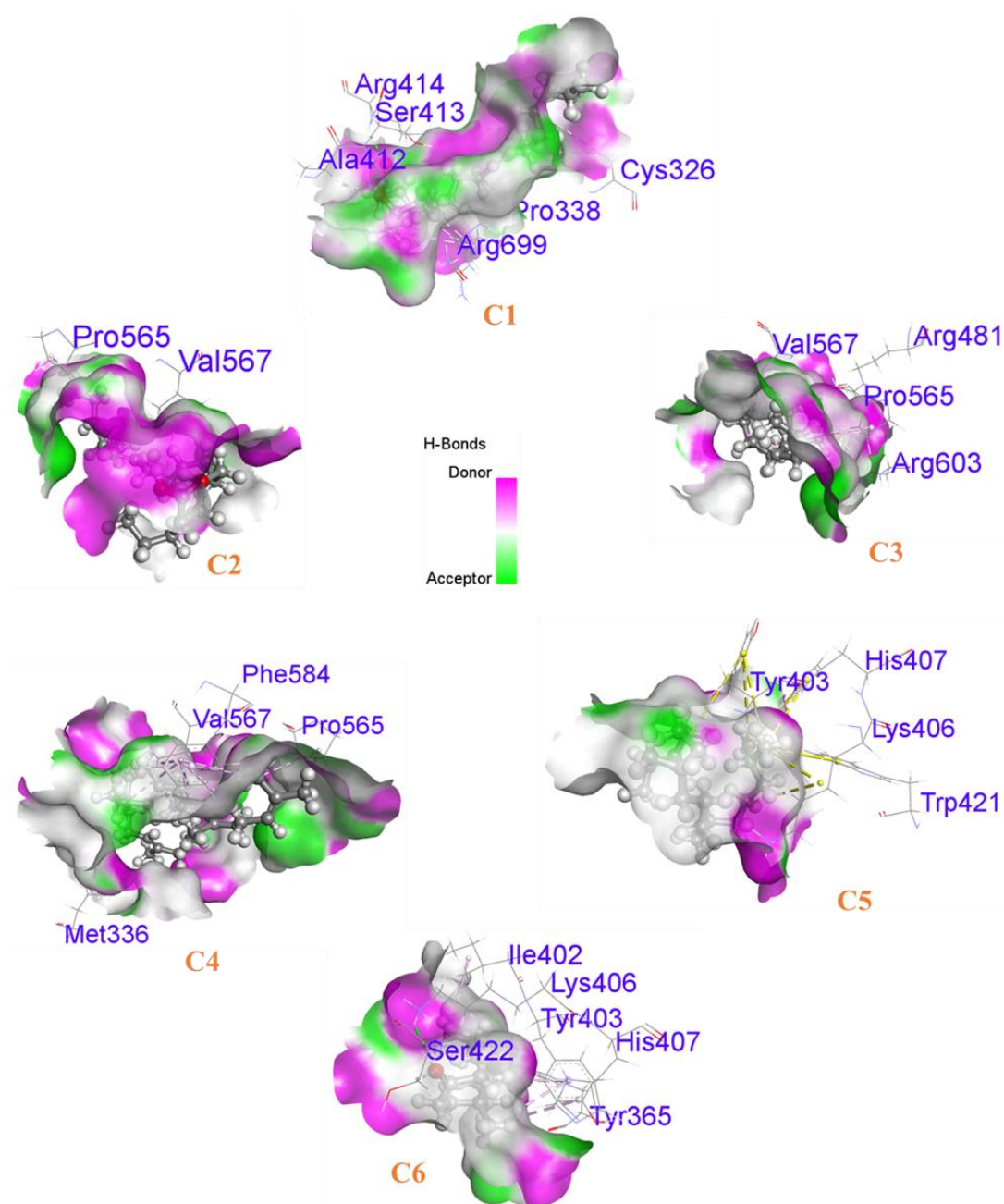
Fig. 5. Hydrogen bond-surface area of the studied compounds with the 6NGJ protein

Noncovalent interactions are essential for medication stability, changes in binding affinity, and therapeutic efficacy (Patil *et al*. 2010). To promote protein-ligand interactions, the H-bond must be strong, and the distance should be equal to or smaller than 2.3 Å (Uzzaman *et al*. 2021). In this investigation, all the molecules contain H-bonds except for C2, C4, and C5. There are three C-H bonds present in AA, C1, and C6 with PHE704 (3.06146 Å), ALA412 (2.49876 Å), and SER422 (2.58701 Å) amino acids, respectively. Herein, the C2 compound is interlinked with HEM801 amino acids via a π-σ bond at a distance of 2.55031 Å. In addition, all the molecules have alkyl (except AA) and π-alkyl interactions (except AA, C1) with various amino acids (Table S9).

Docking and NBI Against 5NN5

The C6 demonstrated the highest binding score (-7.4 kcal/mol) of all the studied compounds, whereas AC displayed a -7.5 kcal/mol binding score. However, C3 has a poor link to the protein due to its low binding score (-4.4 kcal/mol) (Fig. 3). Hence, C3 has two conventional H-bonds with the ARG594 amino acid, and C1 has a C-H bond with HIS717 (2.72409 Å). The standard drug AC has four conventional H-bonds, two C-H bonds, and a π-alkyl bond with numerous amino acids. Furthermore, all the compounds have alkyl and π-alkyl interactions with numerous amino acid residues (Fig. 7).
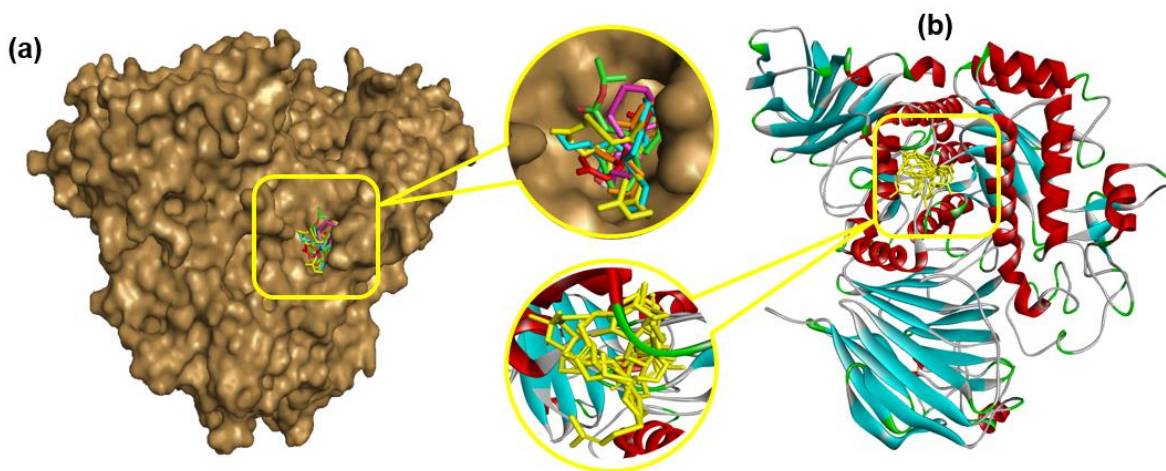

Fig. 6. (a) Surface outlook of the docked conformation of C1 (green), C2 (cyan), C3 (magenta), C4 (yellow), C5 (orange), and C6 (red), and (b) cartoon view of the docked conformation at the binding site of the 5NN5
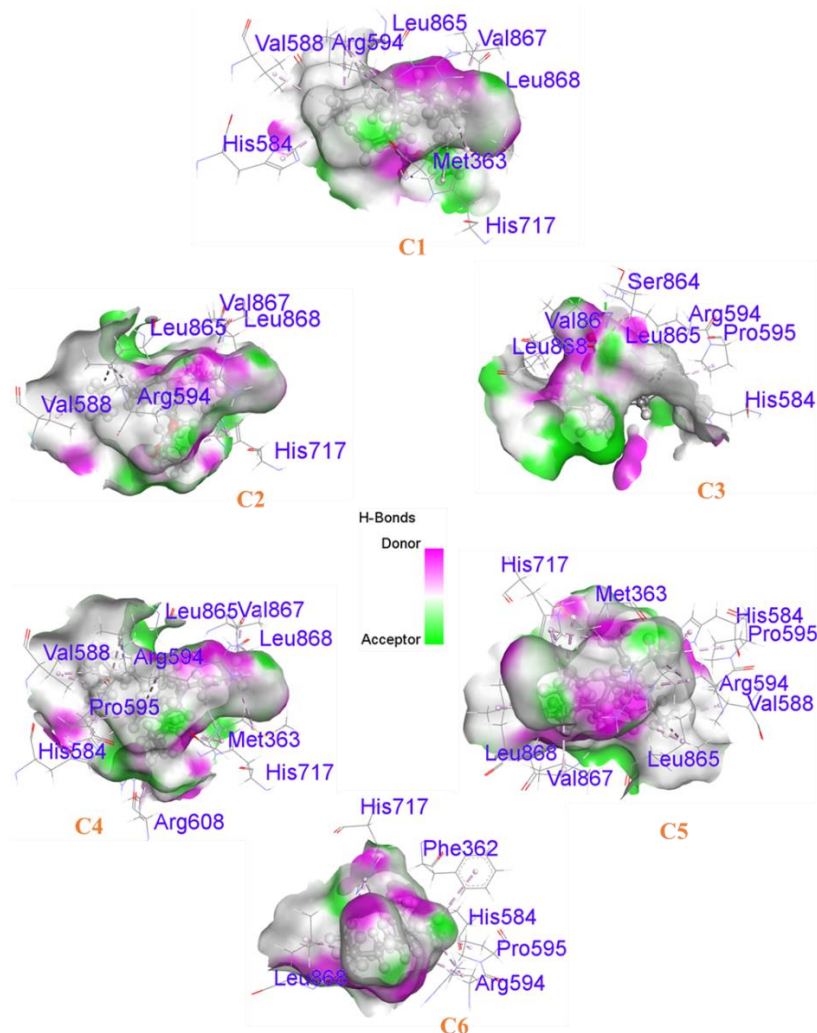
Fig. 7. Hydrogen bond surface area of studied compounds with the 5NN5 protein

Docking and NBI against 4GQR

For antidiabetic action with the α-amylase protein, the C6 chemical had the highest binding score (-7.6 kcal/mol), and C1 binds poorly to the protein (-4.9 kcal/mol) (Fig. 3). The binding score order was AC > C6 > C4 > C2 > C5 > C3 > C1. According to the findings, C2 has a conventional H-bond with ASP300 (2.34645 Å) amino acids, and C1 has two carbon H-bonds with GLU233 (3.07608 Å) and HIS299 (2.42742 Å). On the other hand, π-σ interactions have been discovered in C3 with the amino acid TRP59 at a distance of 2.67916 Å. In addition, all the compounds have alkyl and π-alkyl interactions with numerous amino acid residues, but C6 has no alkyl bond. However, the reference drug AC contains conventional H-bonds and C-H bonds (Fig. 8).
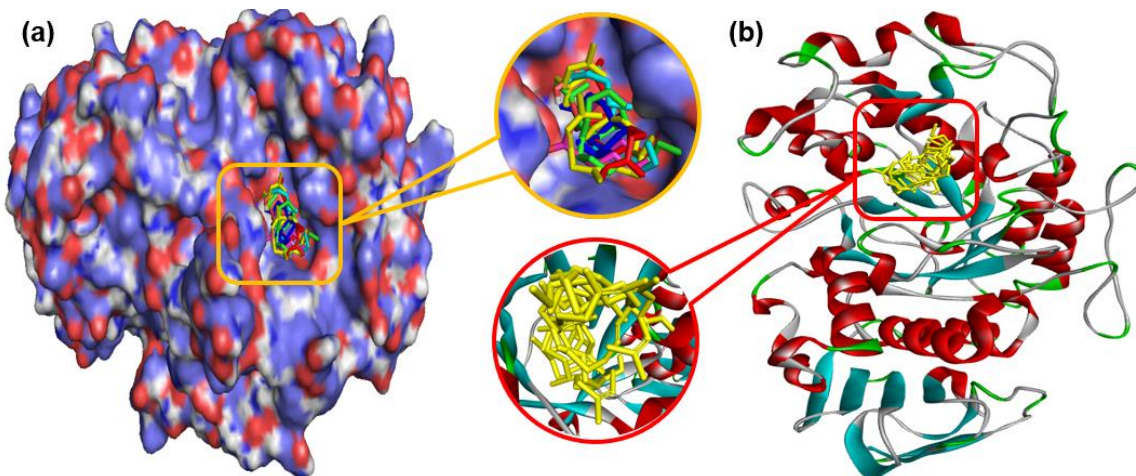
Fig. 8. (a) Surface outlook of the docked conformation of C1 (green), C2 (cyan), C3 (magenta), C4 (yellow), C5 (red), and C6 (blue), and (b) cartoon view of the docked conformation at the binding site of the 4GQR
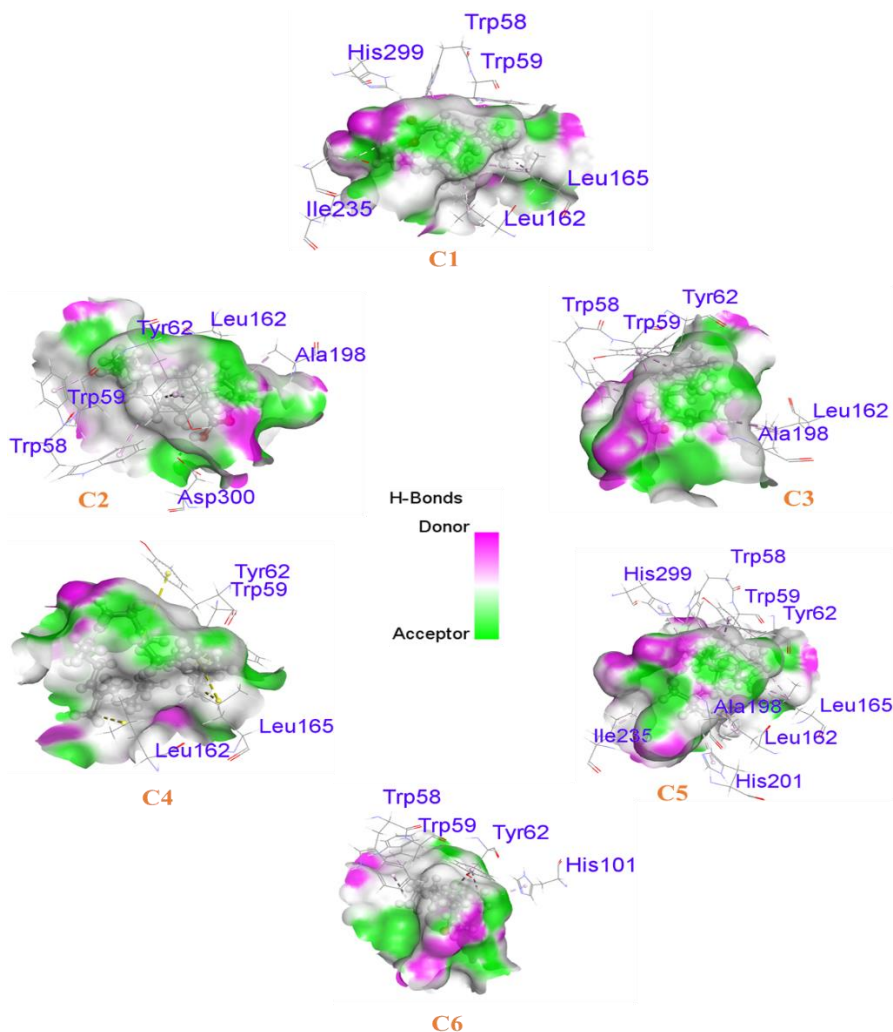

Fig. 8b. Hydrogen bond-surface area of the studied compounds with the 4GQR protein

Molecular Dynamic (MD) Simulation

To understand the relative stability of the complex, the root means square deviations of the simulation trajectories were calculated. Figure 9 (a) specifies that the complex from C6 had a stable profile from the beginning and showed a flexible nature during the passage of 30 ns. The complexes were stable after that and maintained the rigid profile up to 100 ns. The average RMSD of the C4 and C6 complexes were below 2.5 Angstrom, which indicates the strong stable nature of the complex. Additionally, the solvent-accessible surface area of the complexes was evaluated to identify any surface area modifications. The SASA profile in Figs. 9(b) and 10(b) for complexes C4 and C6 indicate that all complexes maintained less deviation throughout the simulation trajectories, which indicates the stable nature of the complex. The radius of gyration of the simulated complexes defines the mobile nature of the complexes, whereas Fig. 9(c) and Fig. 10(c) indicate that C4 and C6 complexes exhibited less deviation. The H-bond from both complexes in Fig. 9(d) and Fig. 10(d) demonstrates the strong binding profile of the complex.
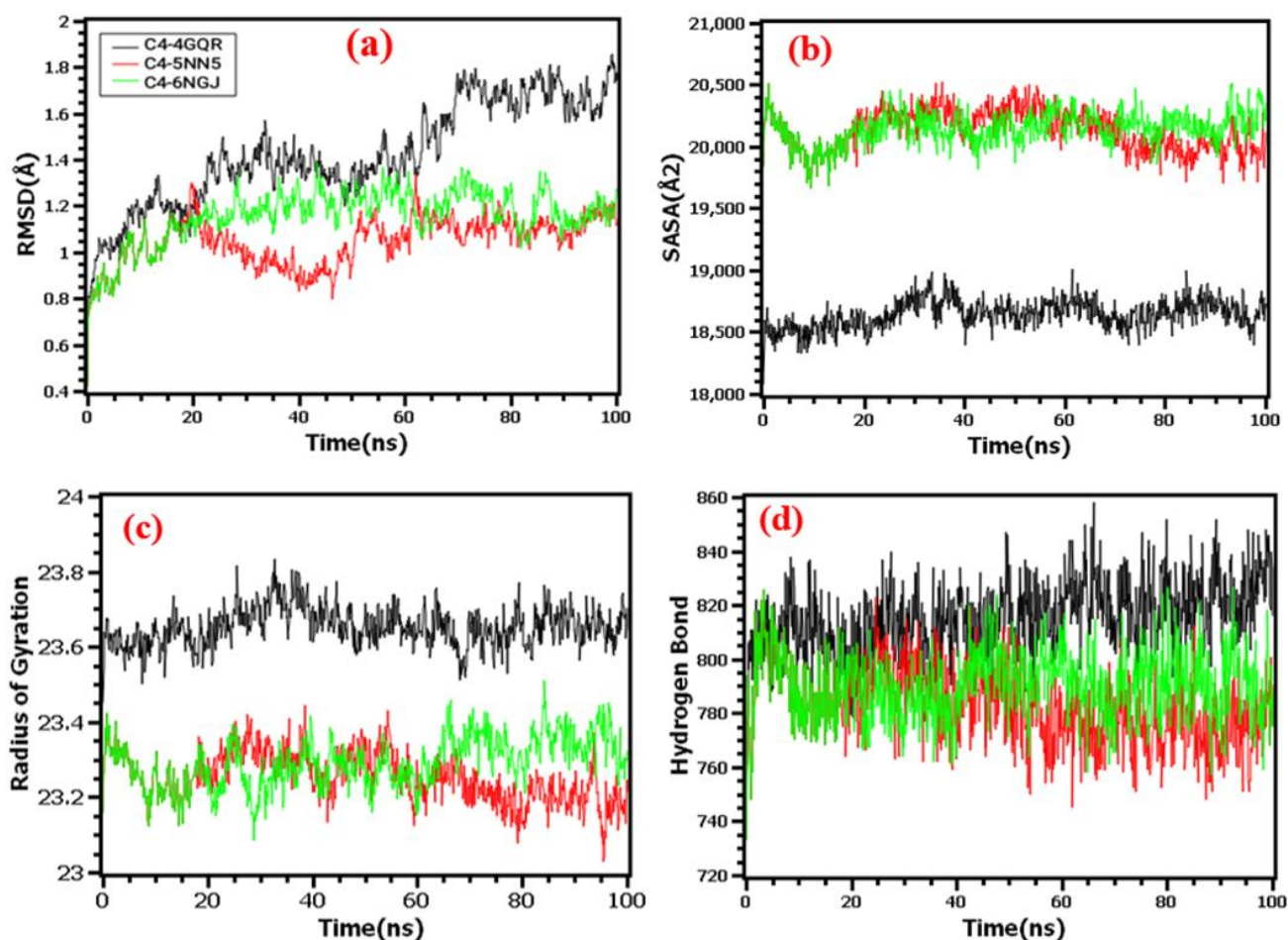

Fig. 9. MD simulation of 6NGJ, 5NN5, and 4GQR proteins in complex with C4 ligand (a) RMSD of docked complexes from α-C atoms. The structural exchanges of receptor protein using (b) SASA, (c) Radius of Gyration (d) number of H-bonds developed, respectively
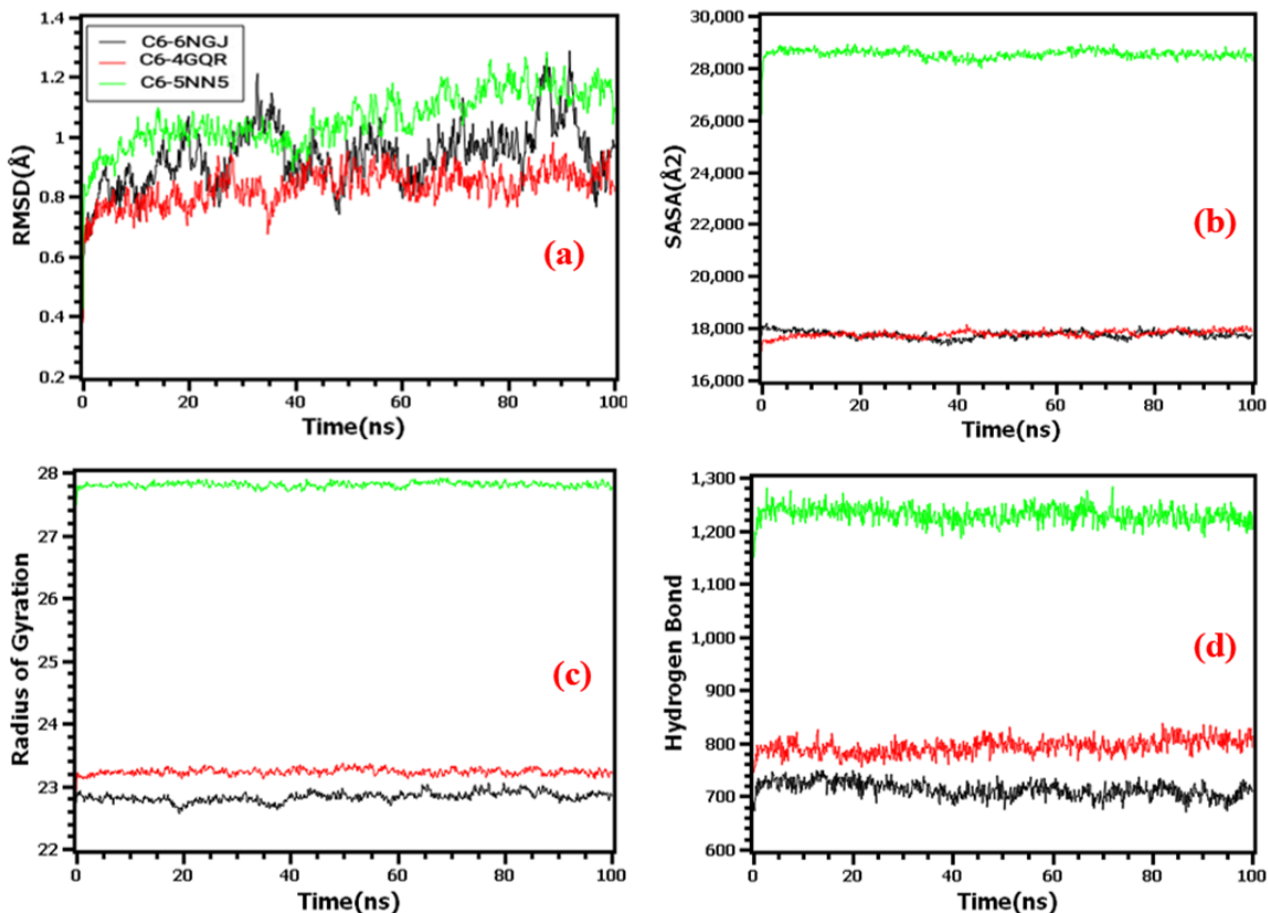
Fig. 10. MD simulation of 6NGJ, 4GQR, and 5NN5 proteins in complex with C6 ligand (a) RMSD of docked complexes from α-C atoms. The structural variations in the receptor protein using (b) SASA, (c) Radius of Gyration (d) number of H-bonds developed respectively.

Pharmacokinetic Analysis

The pharmacokinetic profile analysis is represented in Table 3. According to the study, each chemical exhibits good HIA and CACO-2 permeability. Oral bioavailability is good without AA, C5, and C6 compounds. In addition, the BBB is good with all chemicals. AA, AC, and all discovered medications are noncarcinogenic and have oral toxicity categories III (C1, C2, C4, C5, C6) and IV (AA, AC, and C3) (Li *et al*. 2014). In this study, all medications were p-GP and CYP4502C9 non-inhibitors. On the other hand, AC and C4 have been shown to suppress hERG, which can lengthen the QT interval (Hasan *et al*. 2023).

Biological Activity Prediction

PASS's web server can predict the biological characteristics of several substances (Lagunin *et al*. 2000). Utilizing PASS data, the AA, AC, and six compounds were investigated (Table 4), and their antioxidant activities ranged from 0.222 (C3) to 0.928 (AA). Here, these compounds have anti-inflammatory, α-glucosidase inhibitory, and α-amylase inhibitory effects (except AA). Furthermore, with C4 > C1 > C2 > C5 > C6 > C3 > AA, each molecule possesses anti-ulcerative effects. Moreover, all the compounds exhibited antipruritic (without AC) characteristics, with C2 showing the highest value (0.719). Finally, all the selected compounds demonstrated the aforementioned effects.

Table 3. Pharmacokinetic Analysis

Name	Absorption			Distribution			Metabolism	Toxicity		
	HIA	HOB	C2P	BBB	P-GpI	P-GpS	CYP4502C9	hERG	Carcinogen	AOT
AA	+0.622	+0.586	- 0.976	+0.875-	- 0.972	- 0.968	- 0.938	- 0.784	- 0.970	IV
AC	-0.966	- 0.900	- 0.896	- 0.800	- 0.582	- 0.709	- 0.839	+0.715	- 0.980	IV
C1	+0.997	- 0.643	+0.833	+0.925	- 0.632	- 0.939	- 0.933	- 0.424	- 0.640	III
C2	+0.997	- 0.643	+0.825	+0.925	- 0.689	- 0.939	- 0.933	- 0.453	- 0.640	III
C3	+0.994	- 0.671	+0.711	+0.850	- 0.932	- 0.964	- 0.958	- 0.464	- 0.704	IV
C4	+0.988	- 0.514	+0.700	+1.000	- 0.661	- 0.980	- 0.917	+0.696	- 0.570	III
C5	+0.986	+ 0.529	+0.778	+1.000	- 0.869	- 0.839	- 0.889	- 0.511	- 0.560	III
C6	+0.997	+ 0.714	+0.835	+0.875	- 0.886	- 0.868	- 0.828	- 0.731	- 0.910	III

HOB = Human oral bioavailability, HIA = Human intestinal absorption, BBB = Blood-brain barrier, C2P = CACO-2 permeability, P-GpS = P-glycoprotein substrate, P-GI = P-glycoprotein inhibitor, hERG = human ether a-go-go-gene, AOT = Acute oral toxicity.

Table 4. Biological Activity Prediction of the Selective Compounds

Name	Antioxidant	Anti-inflammation	α-glucosidase inhibitor	α-amylase inhibitor	Antiulcerative	Antipruritic
AA	0.928	0.779	-	-	0.522	0.429
AC	0.351	0.280	0.956	0.943	-	-
C1	0.269	0.700	0.076	0.497	0.663	0.452
C2	0.269	0.700	0.076	0.497	0.663	0.719
C3	0.222	0.515	0.150	0.583	0.525	0.622
C4	0.657	0.701	0.447	0.573	0.676	0.361
C5	0.461	0.286	0.121	0.135	0.585	0.279
C6	0.321	0.681	0.751	0.795	0.532	0.658

CONCLUSIONS

1. The leaf extract and fractions contained alkaloids, flavonoids, phenolic compounds, and other phytochemicals. The quantitative investigation revealed that the ethyl acetate fraction (EFM) had the highest total phenol content (TPC) and total flavonoid content (TFC). In addition, EFM and dichloromethane (DFM) fractions showed the highest total antioxidant content (TAC) with 2,2-diphenyl-1-picrylhydrazyl (DPPH) scavenging activity and ferric-reducing capacity.

2. During the antidiabetic evaluation, the EFM fraction showed a significant inhibitory influence on α-amylase enzymes and α-glucosidase.

3. Furthermore, gas chromatography – mass spectrometry (GC–MS) analysis showed the presence of bioactive phytoconstituents with antipyretic, anti-inflammatory, antioxidant, and antidiabetic properties.

4. Based on molecular docking results, the C4 and C6 compounds would be a valuable source of potential drug candidate for their greatest binding score against antioxidant and antidiabetic proteins.

5. According to dynamic simulation, the complex from C6 exhibited a steady profile from the start and displayed flexibility up until 30 ns periods. After that, the complexes remained stable and kept their stiff profile for 100 ns. The average RMSD of the C4 and C6 complexes was under 2.5Å, indicating the complex's high stability.

6. ADMET results demonstrated that the chosen compounds are noncarcinogenic and well absorbed. The PASS prediction results showed moderate to strong antioxidant, anti-inflammatory, and other actions.

7. These findings suggest that *F. macrophylla* leaf may be a potent herbal medicine source for drug development.

ACKNOWLEDGMENTS

REFERENCES CITED

Abirami, P., and Rajendran, A. (2011). "GC-MS determination of bioactive compounds of *Indigofera aspalathoides*," *J. Nat. Prod. Plant Resour.* 1(4), 126-130.

Alam, U., Asghar, O., Azmi, S., and Malik, R. A. (2014). "General aspects of diabetes mellitus," *Handbook of Clinical Neurology* 126, 211-222.

Ali, M. A., Devi, L. I., Nayan, V., Chanu, K. V., and Ralte, L. (2010). "Antioxidant activity of fruits available in Aizawl market of Mizoram, India," *International*

Journal of Biological and Pharmaceutical 1(2), 76-81.

Alqahtani, A. S., Hidayathulla, S., Rehman, M. T., ElGamal, A. A., Al-Massarani, S., Razmovski-Naumovski, V., Alqahtani, M. S., El Dib, R. A., and AlAjmi, M. F. (2019). "Alpha-amylase and alpha-glucosidase enzyme inhibition and antioxidant potential of 3-oxolupenal and katononic acid isolated from *Nuxia oppositifolia*," *Biomolecules* 10(1), article 61. DOI: 10.3390/biom10010061

Alsolami, A., Bazaid, A. S., Alshammari, M. A., Qanash, H., Amin, B. H., Bakri, M. M., & Abdelghany, T. M. (2023). "Ecofriendly fabrication of natural jojoba nanoemulsion and chitosan/jojoba nanoemulsion with studying the antimicrobial, anti-biofilm, and anti-diabetic activities *in vitro*," *Biomass Conv. Bioref*. DOI: 10.1007/s13399-023-05162-0

Arumugam, G., Manjula, P., and Paari, N. (2013). "A review: Anti diabetic medicinal plants used for diabetes mellitus," *Journal of Acute Disease* 2(3), 196-200.

Bakri, M. M., Alghonaim, M. I., Alsalamah, S. A., Yahya, R. O., Ismail, K. S., & Abdelghany, T. M. (2024). "Impact of moist heat on phytochemical constituents, anti-helicobacter pylori, antioxidant, anti-diabetic, hemolytic and healing properties of rosemary plant extract *in vitro*," *Waste Biomass Valor* DOI: 10.1007/s12649-024-02490-8

Bayero, A. S., Datti, Y., Shuaibu, M. M., Nafisatu, A. M., Asma'u, A. A., Dikko, M. A., Zakari, A. H., and Yusuf, M. (2019). "Phytochemical screening and antibacterial activity of the root bark extracts of *Neocarya macrophylla*," *ChemSearch Journal* 10(2), 41-45.

Begum, A. A., Haque, M. M., Islam, M., and Kundu, S. K. (2013). "Evaluation of antioxidant activity and cytotoxic property of methanolic extract of *Flemingia macrophylla* (Willd.)," *Bangladesh Pharmaceutical Journal* 16(2), 159-163.

Blois, M. S. (1958). "Antioxidant determinations by the use of a stable free radical," *Nature* 181(4617), 1199-1200.

Bodoprost, J., and Rosemeyer, H. (2007). "Analysis of phenacylester derivatives of fatty acids from human skin surface sebum by reversed-phase HPLC: Chromatographic mobility as a function of physico-chemical properties," *International Journal of Molecular Sciences* 8(11), 1111-1124.

Bouyahya, A., Abrini, J., El-Baabou, A., Bakri, Y., and Dakka, N. (2016). "Determination of phenol content and antibacterial activity of five medicinal plants ethanolic extracts from North-West of Morocco," *J. Plant. Pathol. Microbiol.* 7(342), 2.

Brighente, I. M. C., Dias, M., Verdi, L. G., and Pizzolatti, M. G. (2007). "Antioxidant activity and total phenolic content of some Brazilian species," *Pharmaceutical biology* 45(2), 156-161.

Calixto, J. B. (2019). "The role of natural products in modern drug discovery," *Anais da Academia Brasileira de Ciências* 91.

Desmarchelier, C., Novoa Bermudez, M. J., Coussio, J., Ciccia, G., and Boveris, A. (1997). "Antioxidant and prooxidant activities in aqueous extracts of Argentine plants," *International Journal of Pharmacognosy* 35(2), 116-120.

Dey, P., Kundu, A., Kumar, A., Gupta, M., Lee, B. M., Bhakta, T., Dash, S., and Kim, H. S. (2020). "Analysis of alkaloids (indole alkaloids, isoquinoline alkaloids, tropane alkaloids)," in: *Recent Advances in Natural Products Analysis* 505-567.

Do, H. T., Li, H., Chreifi, G., Poulos, T. L., and Silverman, R. B. (2019). "Optimization of blood–brain barrier permeability with potent and selective human neuronal nitric

oxide synthase inhibitors having a 2-aminopyridine scaffold," *Journal of Medicinal Chemistry* 62(5), 2690-2707.

Elya, B., Basah, K., Mun'im, A., Yuliastuti, W., Bangun, A., and Septiana, E. K. (2012). "Screening of α-glucosidase inhibitory activity from some plants of Apocynaceae, Clusiaceae, Euphorbiaceae, and Rubiaceae," *Journal of Biomedicine and Biotechnology* 2012.

Filimonov, D. A., Lagunin, A. A., Gloriozova, T. A., Rudik, A. V, Druzhilovskii, D. S., Pogodin, P. V, and Poroikov, V. V. (2014). "Prediction of the biological activity spectra of organic compounds using the PASS online web resource," *Chemistry of Heterocyclic Compounds* 50(3), 444-457.

Fındık, E., Ceylan, M., and Elmastaş, M. (2011). "Isoeugenol-based novel potent antioxidants: Synthesis and reactivity," *European Journal of Medicinal Chemistry* 46(9), 4618-4624.

Gomathi, D., Kalaiselvi, M., Ravikumar, G., Devaki, K., and Uma, C. (2015). "GC-MS analysis of bioactive compounds from the whole plant ethanolic extract of *Evolvulus alsinoides* (L.) L," *Journal of Food Science and Technology* 52, 1212-1217.

Guan, L., Yang, H., Cai, Y., Sun, L., Di, P., Li, W., Liu, G., and Tang, Y. (2019). "ADMET-score–a comprehensive scoring function for evaluation of chemical drug-likeness," *MedChemComm* 10(1), 148-157.

Hasan, M. K., Akhter, S., Fatema, K., Hossain, M. R., Sultana, T., and Uzzaman, M. (2023). "Selective modification of diclofenac to reduce the adverse effects; A computer-aided drug design approach," *Informatics in Medicine Unlocked* 36, article 101159. DOI: 10.1016/j.imu.2023.101159

Iriti, M., and Faoro, F. (2008). "Oxidative stress, the paradigm of ozone toxicity in plants and animals," *Water, Air, and Soil Pollution* 187(1), 285-301.

Jan, S., Khan, M. R., Rashid, U., and Bokhari, J. (2013). "Assessment of antioxidant potential, total phenolics and flavonoids of different solvent fractions of *Monotheca buxifolia* fruit," *Osong Public Health and Research Perspectives* 4(5), 246-254.

Jannat, N., Fatema, K., Haque, M. A., Fatema, J., Rahman, M., Shimu, M. S. S., and Uzzaman, M. (2024). "Evaluation of the antioxidant, thrombolytic, and antimicrobial effects of *Corchorus aestuans* L. leaf extracts: an in-vitro and in-silico study," *South African Journal of Botany* 164, 322-333. DOI: 10.1016/j.sajb.2023.11.045

John, B., Sulaiman, C. T., George, S., and Reddy, V. R. K. (2014). "Total phenolics and flavonoids in selected medicinal plants from Kerala," *International Journal of Pharmacy and Pharmaceutical Sciences* 6(1), 406-408.

Kabir, M. S. H., Habib, I. Bin, Hossain, M. K., Khan, E., Samrat, M. N. H. J., Uddin, S. M., Ahmed, M., Chowdhury, M. S. C., Hasanat, A., and Rahman, M. M. (2015). "*In silico* pass prediction and molecular docking of isolated compounds from *Flemingia macrophylla* for thrombolytic effect," *World Journal of Pharmaceutical Research* 5990(2), 274-283.

Kala, S. M. J., Balasubramanian, T., Soris, P. T., and Mohan, V. R. (2011). "GC-MS determination of bioactive components of *Eugenia singampattiana* Bedd," *International Journal of ChemTech Research* 3(3), 1534-1537.

Kasangana, P. B., Haddad, P. S., and Stevanovic, T. (2015). "Study of polyphenol content and antioxidant capacity of *Myrianthus arboreus* (Cecropiaceae) root bark extracts," *Antioxidants* 4(2), 410-426.

Kifle, Z. D., Debeb, S. G., and Belayneh, Y. M. (2021). "*In vitro* α-amylase and α-glucosidase inhibitory and antioxidant activities of the crude extract and solvent

fractions of *Hagenia abyssinica* leaves," *BioMed Research International* 2021. DOI: 10.1155/2021/6652777

Krieger, E., and Vriend, G. (2015). "New ways to boost molecular dynamics simulations," *Journal of Computational Chemistry* 36(13), 996-1007.

Kumar, S., Sandhir, R., and Ojha, S. (2014). "Evaluation of antioxidant activity and total phenol in different varieties of *Lantana camara* leaves," *BMC Research Notes* 7(1), 1–9.

Kupchan, S. M., and Tsou, G. (1973). "Tumor inhibitors. LXXXI. Structure and partial synthesis of fabacein," *The Journal of Organic Chemistry* 38(5), 1055-1056.

Kwon, Y., Apostolidis, E., and Shetty, K. (2008). "Inhibitory potential of wine and tea against α-amylase and α-glucosidase for management of hyperglycemia linked to type 2 diabetes," *Journal of Food Biochemistry* 32(1), 15-31.

Lagunin, A., Stepanchikova, A., Filimonov, D., and Poroikov, V. (2000). "PASS: Prediction of activity spectra for biologically active substances," *Bioinformatics* 16(8), 747-748.

Lengauer, T., and Rarey, M. (1996). "Computational methods for biomolecular docking," *Current Opinion in Structural Biology* 6(3), 402-406.

Lou, S., Yu, Z., Huang, Z., Wang, H., Pan, F., Li, W., Liu, G., and Tang, Y. (2024). "In silico prediction of chemical acute dermal toxicity using explainable machine learning methods," *Chemical Research in Toxicology* 37(3), 513-524. DOI: 10.1021/acs.chemrestox.4c00012

Mujeeb, F., Bajpai, P., and Pathak, N. (2014). "Phytochemical evaluation, antimicrobial activity, and determination of bioactive components from leaves of *Aegle marmelos*," *BioMed Research International* 2014.

Odeja, O., Ogwuche, C. E., Elemike, E. E., and Obi, G. (2017). "Phytochemical screening, antioxidant and antimicrobial activities of *Acalypha ciliata* plant," *Clinical Phytoscience* 2(1), 1-6.

Oyaizu, M. (1986). "Studies on products of browning reaction antioxidative activities of products of browning reaction prepared from glucosamine," *The Japanese Journal of Nutrition and Dietetics* 44(6), 307-315.

Patel, S. S., and Savjani, J. K. (2015). "Systematic review of plant steroids as potential antiinflammatory agents: Current status and future perspectives," *The Journal of Phytopharmacology* 4(2), 121-125.

Patil, R., Das, S., Stanley, A., Yadav, L., Sudhakar, A., and Varma, A. K. (2010). "Optimized hydrophobic interactions and hydrogen bonding at the target-ligand interface leads the pathways of drug-designing," *PloS One* 5(8), article e12029.

Prieto, P., Pineda, M., and Aguilar, M. (1999). "Spectrophotometric quantitation of antioxidant capacity through the formation of a phosphomolybdenum complex: Specific application to the determination of vitamin E," *Analytical Biochemistry* 269(2), 337-341.

Rahman, F., Patwary, M. A. M., Siddique, M. A. B., Bashar, M. S., Haque, M. A., Akter, B., Rashid, R., Haque, M. A., and Uddin, A. K. M. R. (2022). "Green synthesis of ZnO nanoparticles using Cocos nucifera leaf extract: Characterization, antimicrobial, antioxidant, and photocatalytic activity," *Royal Society Open Science* 9, article 220858.

Rahman, M., Islam, M., Biswas, M., and Khurshid Alam, A. H. M. (2015). "In vitro antioxidant and free radical scavenging activity of different parts of *Tabebuia pallida* growing in Bangladesh," *BMC Research Notes* 8(1), 1-9.

Roig-Zamboni, V., Cobucci-Ponzano, B., Iacono, R., Ferrara, M. C., Germany, S., Bourne, Y., Parenti, G., Moracci, M., and Sulzenbacher, G. (2017). "Structure of human lysosomal acid α-glucosidase–A guide for the treatment of Pompe disease," *Nature Communications* 8(1), article 1111.

Rose, P. W., Prlić, A., Altunkaya, A., Bi, C., Bradley, A. R., Christie, C. H., Costanzo, L. Di, Duarte, J. M., Dutta, S., and Feng, Z. (2016). "The RCSB protein data bank: Integrative view of protein, gene and 3D structural information," *Nucleic Acids Research* gkw1000.

Rupa, S. A., Ghann, W. E., Patwary, M. A. M., and Uddin, J. (2022). "Highly selective naked eye pyridine-2, 6-dicarbohydrazide based colorimetric and fluorescence chemosensor for Pb^{2+} with AIE activity," *Inorganic Chemistry Communications* 144, article 109937.

Shahadat, S., Tareq, S. M., Chowdhury, M. M. U., and Ahsan, M. Q. (2015). "In-vivo analgesic, antipyretic potential in Swiss albino mice and in-vitro anti-inflammatory evaluation of *Flemingia macrophylla* (Willd)," *International Journal of Pharmacognosy and Phytochemistry* 30(1), 1308-1312.

Sure, R., Antony, J., and Grimme, S. (2014). "Blind prediction of binding affinities for charged supramolecular host–guest systems: achievements and shortcomings of DFT-D3," *The Journal of Physical Chemistry B* 118(12), 3431-3440.

Syiem, D., and Khup, P. Z. (2007). "Evaluation of *Flemingia macrophylla* L., a traditionally used plant of the northeastern region of India for hypoglycemic and anti-hyperglycemic effect on mice," *Pharmacologyonline* 2, 355-366.

Tripathi, I. P., and Mishra, C. (2015). "Phytochemical screening of some medicinal plants of Chitrakoot region," *Indian Journal of Applied Research* 5(12), 56-60.

Umesha, S., Marahel, S., and Aberomand, M. (2013). "Antioxidant and antidiabetic activities of medicinal plants: A short review," *International Journal of Research in Phytochemistry and Pharmacology* 3(1), 40-53.

Uzzaman, M., Fatema, K., Akhter, S., Hossain, M. R., Akter, N., Tasnuva, S., Jahan, S., Hasan, M. K., Shimu, M. S. S., Hossain, M. K., and Afrin, M. F. (2023). "Medicinal and toxicological investigation of some common NSAIDs; A computer-aided drug design approach," *Journal of Molecular Structure* 1292, article 136124. DOI: 10.1016/j.molstruc.2023.136124

Uzzaman, M., Hasan, M. K., Mahmud, S., Fatema, K., and Matin, M. M. (2021). "Structure-based design of new diclofenac: Physicochemical, spectral, molecular docking, dynamics simulation and ADMET studies," *Informatics in Medicine Unlocked* 25. DOI: 10.1016/j.imu.2021.100677

Williams, L. K., Li, C., Withers, S. G., and Brayer, G. D. (2012). "Order and disorder: differential structural impacts of myricetin and ethyl caffeate on human amylase, an antidiabetic target," *Journal of Medicinal Chemistry* 55(22), 10177-10186.

Wolfe, K., Wu, X., and Liu, R. H. (2003). "Antioxidant activity of apple peels," *Journal of Agricultural and Food Chemistry* 51(3), 609-614.